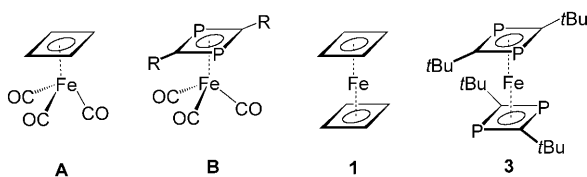


A Phosphorus Analogue of Bis(η^4 -cyclobutadiene)iron(0)**

Robert Wolf, J. Chris Slootweg, Andreas W. Ehlers, František Hartl, Bas de Bruin, Martin Lutz, Anthony L. Spek, and Koop Lammertsma*

Iron is a pivotal element in organometallic chemistry, enabling fundamental insights with high-impact applications.^[1] Ferrocene derivatives have countless uses,^[2] and the recent advances in iron catalysis are equally impressive.^[3]

A historic landmark in organoiron chemistry is (η^4 -cyclobutadiene)iron tricarbonyl, $[\text{Fe}(\eta^4\text{-C}_4\text{H}_4)(\text{CO})_3]$ (**A**).



This molecule was predicted on theoretical grounds^[4] and synthesized by Pettit and co-workers,^[5,6] and it undergoes electrophilic substitutions similar to ferrocene.^[7] Still, the number of cyclobutadiene (Cb) iron complexes pales in comparison to the wealth of iron complexes with the ubiquitous cyclopentadienyl (Cp) ring.^[8] This imbalance is also found for the even less developed phosphaorganometal-

lic complexes of iron. For example, whereas the P_2 analogue of **A**, $[\text{Fe}(\eta^4\text{-P}_2\text{C}_2\text{R}_2)(\text{CO})_3]$ (**B**; R = *t*Bu, Mes), is readily prepared by reaction of $\text{RC}\equiv\text{P}$ with $[\text{Fe}_2(\text{CO})_9]$,^[9] iron sandwich complexes with phosphacyclobutadienes remain essentially limited to neutral, heteroleptic species,^[10,11] thereby sharply contrasting the well-developed phosphaferrocenes used in areas ranging from catalysis to supramolecular chemistry.^[12,13]

Illustrative of the dichotomy in Cp and Cb iron sandwich compounds is the still-elusive 16-electron complex bis(η^4 -cyclobutadiene)iron(0), $[\text{Fe}(\eta^4\text{-C}_4\text{H}_4)_2]$ (**1**),^[14] which DFT calculations indicate to have a stable D_{4h} -symmetric structure (Figure 1) with a triplet ground state (see below).^[15] In our pursuit of this system we make use of the C/P diagonal relationship in the Periodic Table.

Recently, we showed that reaction of phosphaalkynes with anionic arene complexes of low-valent transition metals is a facile method to prepare homoleptic diphosphacyclobutadiene sandwich anions, such as the diamagnetic 18-electron ion $[\text{Co}(\eta^4\text{-P}_2\text{C}_2\text{tBu}_2)_2]^-$, which displays a unique reactivity pattern with electrophiles.^[16] We now report on the synthesis and structural characterization of the d^9 17-electron anionic iron complex $[\text{Fe}(\eta^4\text{-P}_2\text{C}_2\text{tBu}_2)_2]^-$ (**2**) and the neutral d^8 16-electron $[\text{Fe}(\eta^4\text{-P}_2\text{C}_2\text{tBu}_2)_2]$ (**3**) as a phosphorus analogue of homoleptic $[\text{Fe}(\eta^4\text{-C}_4\text{H}_4)_2]$ (**1**).

$[\text{K}([18]\text{crown-6})(\text{thf})_2][\text{Fe}(\eta^4\text{-P}_2\text{C}_2\text{tBu}_2)_2]$ (**K 2**) was prepared as a yellow-orange solid from the metalate $[\text{K}([18]\text{crown-6})(\text{thf})_2][\text{Fe}(\eta^4\text{-C}_{14}\text{H}_{10})_2]$ ^[17a] and four equivalents $\text{tBuC}\equiv\text{P}$ ^[18] in 75% yield. The X-ray crystal structure (Figure 2)^[19] is comprised of the counterion $[\text{K}([18]\text{crown-6})(\text{thf})_2]^+$ ^[17b] and the homoleptic anion $[\text{Fe}(\eta^4\text{-P}_2\text{C}_2\text{tBu}_2)_2]^-$ (**2**). The Fe–P and Fe–C separations in **2** are comparable to those in complex **B**^[9,10] and are slightly longer (by 0.03–0.04 Å) than the Co–P and Co–C separations in the isomorphous complex $[\text{K}([18]\text{crown-6})(\text{thf})_2][\text{Co}(\eta^4\text{-P}_2\text{C}_2\text{tBu}_2)_2]$.^[16] The two η^4 -bound $\text{P}_2\text{C}_2\text{tBu}_2$ ligands in the anion are in a staggered orientation.

Anion **2** is a paramagnetic d^9 17-electron species with a solution magnetic moment of $1.77\mu_\text{B}$, indicating the presence of one unpaired electron. In full agreement, the EPR spectrum of a frozen THF solution of **K 2** (40 K) shows the typical pattern for an axially symmetric d^9 species; a satisfactory spectral simulation was obtained with the *g* values $g_{\parallel}=2.28$ and $g_{\perp}=2.026$ (Figure 3).

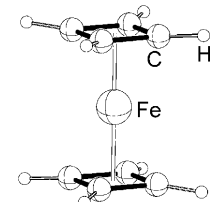


Figure 1. OPBE/TZ2P structure of **1** (D_{4h} symmetry). Bond lengths [Å]: Fe–C 2.007, C–C 1.462, C–H 1.085.

[*] Dr. R. Wolf, Dr. J. C. Slootweg, Dr. A. W. Ehlers, Prof. Dr. K. Lammertsma
Department of Organic and Inorganic Chemistry
Faculty of Sciences, VU University Amsterdam
De Boelelaan 1083, 1081 HV, Amsterdam (The Netherlands)
Fax: (+31) 20-598-7488
E-mail: k.lammertsma@few.vu.nl

Dr. R. Wolf
Institute of Inorganic and Analytical Chemistry
University of Münster
Corrensstrasse 30, 48149 Münster (Germany)
Dr. F. Hartl, Dr. B. de Bruin
Homogeneous and Supramolecular Catalysis
Van't Hoff Institute for Molecular Sciences
University of Amsterdam
Nieuwe Achtergracht 166, 1018 WV Amsterdam (The Netherlands)
Dr. M. Lutz, Prof. Dr. A. L. Spek
Bijvoet Center for Biomolecular Research
Crystal and Structural Chemistry, Utrecht University
Padualaan 8, 3584 CH, Utrecht (The Netherlands)

[**] Financial support from the Deutsche Forschungsgemeinschaft and the Fonds der Chemischen Industrie (R.W.), the Netherlands Organization for Scientific Research NWO-CW (M.L., A.L.S., B.B.), and Thermphos International BV is gratefully acknowledged. We thank Dr. Gé van Albada (University of Leiden) and Prof. Dr. Dietrich Gudat (University of Stuttgart) for experimental assistance. R.W. thanks Prof. Dr. W. Uhl for his support.

Supporting information for this article is available on the WWW under <http://dx.doi.org/10.1002/anie.200805193>.

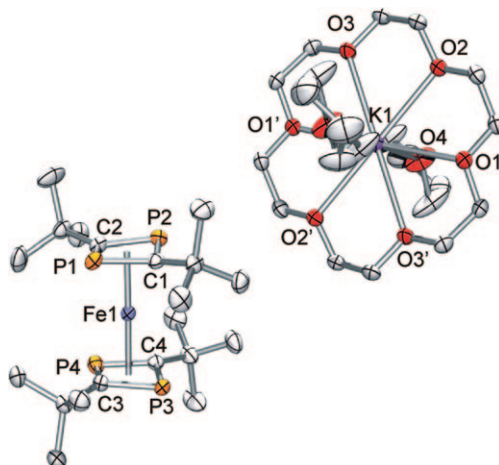


Figure 2. Solid-state structure of **K2**, with displacement ellipsoids at the 50% probability level. H atoms, one of the two crystallographically independent $[K([18]\text{crown-6})(\text{thf})_2]^+$ cations, and the disorder in the thf molecules are omitted for clarity. Selected bond lengths [Å] and angles [$^\circ$]: Fe1–P1, P2, P3, P4 2.2969(5)–2.3024(5), Fe1–C1, C2, C3, C4 2.0939(16)–2.1027(16), P1–C1 1.8000(17), P1–C2 1.8024(17), P2–C1 1.8043(17), P2–C2 1.8021(18), P3–C3 1.8048(17), P3–C4 1.8037(18), P4–C3 1.8042(17), P4–C4 1.8013(17); P1–C1–P2 98.72(8), C1–P1–C2 80.94(8).

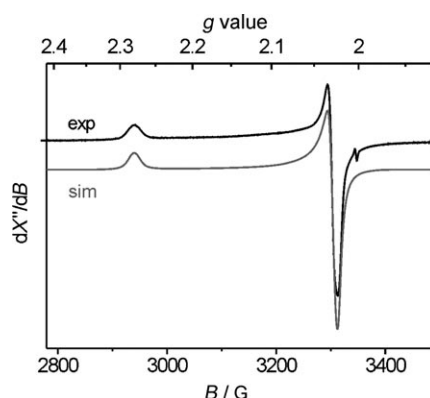


Figure 3. Experimental EPR spectrum of **K2** and its simulation. Microwave frequency 9.38028 GHz, attenuation 30 dB, modulation amplitude 4 G.

The absence of hyperfine coupling and the high-field shift of g_{\parallel} compared to g_{\perp} indicate that the unpaired electron is localized in the $d_{x^2-y^2}$ orbital of the metal.^[20] This conclusion is supported by a molecular orbital analysis of model complex ion $[\text{Fe}(\eta^4-\text{P}_2\text{C}_2\text{Me}_2)_2]^-$ (**2'**, with methyl instead of *tert*-butyl groups), which shows an 84 % metal $d_{x^2-y^2}$ contribution in the singly occupied molecular orbital (SOMO), while the highest doubly occupied orbital displays 79 % d_{z^2} character. The OPBE/TZ2P DFT calculations^[15] give a significant energetic preference for the doublet state over both the quartet ($\Delta E = 30.4 \text{ kcal mol}^{-1}$) and the sextet ($\Delta E = 64.0 \text{ kcal mol}^{-1}$).

To establish whether **2** is a suitable precursor for the oxidized neutral complex $[\text{Fe}(\eta^4-\text{P}_2\text{C}_2\text{tBu}_2)_2]$ (**3**) or the reduced 18-electron dianion $[\text{Fe}(\eta^4-\text{P}_2\text{C}_2\text{tBu}_2)_2]^{2-}$ (**4**), we examined the redox properties of **K2** (in THF solution) with electrochemical methods. Cyclic voltammetry revealed

anion **2** to be oxidized fully reversibly at a rather low potential, $E_{1/2} = -0.97 \text{ V}$ vs. $[\text{Cp}_2\text{Fe}]/[\text{Cp}_2\text{Fe}]^+$ ^[21] but no reduction of **2** was observed in the accessible potential window. UV/Vis monitoring of the oxidation of **K2** in a thin-layer spectroelectrochemical cell showed smooth conversion to a new species (Figure 4) that was identified as oxidized complex **3** by comparison of the UV/Vis absorptions with those of an authentic sample.

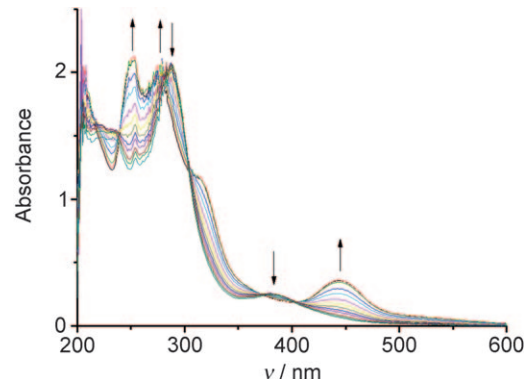


Figure 4. UV/Vis spectral changes accompanying the electrochemical oxidation of **K2** in $\text{THF}/[n\text{Bu}_4\text{N}][\text{PF}_6]$ at -0.9 V . The arrows indicate decreasing absorptions of **K2** and increasing absorptions of **3**.

On a preparative scale, **3** was generated by oxidizing **K2** with $[\text{Cp}_2\text{Fe}][\text{PF}_6]$ to give, upon isolation, deep red crystals that are highly soluble in hydrocarbon solvents. The X-ray crystal structure of neutral, 16-electron **3** (Figure 5) revealed a C_2 -symmetric sandwich structure akin to anion **2**.^[19] It is evident that no major structural change occurs upon oxidation.

The effective magnetic moment in C_6D_6 solution ($2.74 \mu_\text{B}$) indicates that **3** is paramagnetic with two unpaired electrons per molecule. Accordingly, the ^1H NMR spectrum of **3** features a very broad singlet at $\delta = 2.6 \text{ ppm}$ owing to the paramagnetism of the compound.

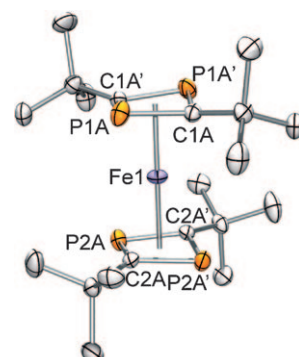


Figure 5. Solid-state structure of **3**, with displacement ellipsoids at the 50% probability level. H atoms and the minor disorder components of the $\text{P}_2\text{C}_2\text{tBu}_2$ ligands are omitted for clarity. Selected bond lengths [Å] and angles [$^\circ$]: Fe1–P1A 2.3044(10), Fe1–P2A 2.3081(9), Fe1–C1A 2.090(3), Fe1–C2A 2.100(3), P1A–C1A 1.804(3), P1A–C1A' 1.808(3), P2A–C2A 1.802(3), P2A–C2A' 1.796(3), P1A–C1A–P1A' 97.98(15), C1A–P1A–C1A' 81.41(15); P2A–C2A–P2A' 98.61(15), C2A–P2A–C2A' 80.91(15).

OPBE/TZ2P geometry optimization of model $[\text{Fe}(\eta^4\text{-P}_2\text{C}_2\text{Me}_2)_2]$ (**3'**, D_{2d} symmetry) gave structural parameters similar to **3**. The triplet ground state of **3'** is favored over the open-shell singlet and the quintet by 20.0 and 37.6 kcal mol⁻¹, respectively. The two singly occupied MOs of the ground state display dominant contributions of the iron orbitals (SOMO-1: 65% d_{z^2} , SOMO: 65% $d_{x^2-y^2}$; Figure 6). Thus,

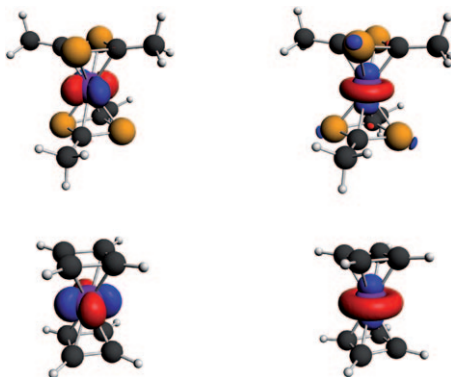


Figure 6. Graphical representations of the SOMO (left) and SOMO-1 (right) of $[\text{Fe}(\eta^4\text{-C}_4\text{H}_4)_2]$ (**1**, bottom) and $[\text{Fe}(\eta^4\text{-P}_2\text{C}_2\text{Me}_2)_2]$ (**3'**, top).

oxidizing **2** results in an open-shell sandwich complex **3** with two unpaired electrons. The oxidized compound **3** displays a similar electronic structure as **2**, but with one electron formally removed from its d_{z^2} -like HOMO.

Formal addition of one electron to model anion **2'** results in the diamagnetic 18-electron dianion $[\text{Fe}(\eta^4\text{-P}_2\text{C}_2\text{Me}_2)_2]^{2-}$ (**4'**). Whereas the theoretical calculations indicate **4'** to be a viable species, no reduction of **K2** could be observed, neither by cyclic voltammetry nor preparatively by using strong reducing agents such as potassium/graphite or potassium/naphthalenide.^[21] We attribute this apparent lack of reduction to the large energy difference between the $d_{x^2-y^2}$ -like HOMO of **4'** (+5.19 eV) and the SOMO of **2'** (0.93 eV), which is caused by the double negative charge.

The DFT calculations reveal a close electronic relationship between the cyclobutadiene sandwich complex $[\text{Fe}(\eta^4\text{-C}_4\text{H}_4)_2]$ (**1**, D_{4h}) and **3'**. Like **3'**, the triplet ground state of **1** is also highly favored over the open-shell singlet ($\Delta E = 20.7$ kcal mol⁻¹) and the quintet ($\Delta E = 47.3$ kcal mol⁻¹). Likewise, the two singly occupied MOs of the ground state of **1** show dominant contributions of the iron atom (SOMO: 88% $d_{x^2-y^2}$, SOMO-1: 82% d_{z^2} ; Figure 6). The Mulliken spin population analysis confirms that the unpaired electron density of both resides almost exclusively on the iron center (net spin density polarization on Fe **1**: 2.42 and **3'**: 2.39 versus **2'**: 1.32). The calculations also show that the bond strength of -106.5 kcal mol⁻¹ for a cyclobutadiene ligand of **1** is higher than that of a diphenylcyclobutadiene ligand of **3'** (-98.7 kcal mol⁻¹) and further that the dimerization energy of acetylene to form cyclobutadiene ($\Delta E = -20.5$ kcal mol⁻¹) exceeds that of MeC≡P ($\Delta E = -12.5$ kcal mol⁻¹). Therefore, from a thermodynamic point of view it appears that the formation of **1** is similarly favorable to that of **3'**.

In summary, the new 17-electron species **2** and 16-electron species **3** are rare examples of readily accessible, open-shell iron sandwich complexes with phosphaorganic ligands. The presented data lead us to conclude that phosphorus derivative **3** is a true analogue of the elusive bis(η^4 -cyclobutadiene)iron(0) compound **1**. Currently, we are investigating whether **1** and its derivatives are likewise accessible. Future studies will focus on a more detailed characterization of the iron oxidation state in **1-3** and the influence of metal coordination on the magnetic and redox properties of these compounds.^[22]

Experimental Section

K2: *t*BuC≡P (5 mL, 10.0 mmol, 2 M solution in hexanes) was added dropwise to a deep brown solution of $[\text{K}([\text{18}] \text{crown}-6)(\text{thf})_2][\text{Fe}(\text{C}_{14}\text{H}_{10})_2]$ (2.13 g, 2.48 mmol) in THF (40 mL) at -78°C, and the mixture was allowed to warm up to room temperature overnight. The dark orange solution was filtered and concentrated to 10 mL, and toluene (30 mL) was added. $[\text{K}([\text{18}] \text{crown}-6)(\text{thf})_2][\text{Fe}(\text{P}_2\text{C}_2\text{Bu}_2)_2]$ was isolated as a yellow-orange crystalline solid after storage at -20°C overnight, washed with toluene (3 × 15 mL), and dried in vacuo. Crystals suitable for X-ray crystallography were grown by layering a THF solution of **K2** with *n*-pentane. Yield 1.41 g (75%). Elemental analysis (%) calcd for $\text{C}_{32}\text{H}_{60}\text{O}_6\text{P}_4\text{FeK}$ ($M = 759.66$): C 50.59, H 7.96; found: C 49.74, H 7.95; m.p. > 300°C (slow dec). ¹H NMR (250.13 MHz, $[\text{D}_8]\text{THF}$): $\delta = -1.9$ (very br s; *t*Bu), 1.73 (br s; THF), 3.72 ppm (br s; THF). Magnetic susceptibility (Evans method, 25°C, $[\text{D}_8]\text{THF}$): $\mu_{\text{eff}} = 1.77 \mu_B$. UV/Vis (THF) λ_{max} [nm] (ϵ [mol⁻¹ dm³ cm⁻¹]): 296 (48100), 383 (10000), 699 (310).

3: $[\text{Cp}_2\text{Fe}][\text{PF}_6]$ (0.050 g, 0.15 mmol) was added to a dark orange solution of **K2** (0.106 g, 0.14 mmol) in THF (6 mL), and the mixture was stirred at room temperature overnight. The solvent was removed completely, the ferrocene byproduct was removed by sublimation (10^{-2} torr, 50°C), and the dark residue was extracted into *n*-pentane (10 mL). Concentrating the orange-red extract to approximately 1 mL yielded red X-ray quality crystals of **3** after storage at -20°C for several days. Yield 0.023 g (36%); m.p. 184–186°C (dark oil). ¹H NMR (250.13 MHz, C_6D_6): $\delta = 2.6$ ppm (very br s; *t*Bu). Magnetic susceptibility (Evans method, 25°C, C_6D_6): $\mu_{\text{eff}} = 2.74 \mu_B$. UV/Vis (THF) λ_{max} [nm] (ϵ [mol⁻¹ dm³ cm⁻¹]): 275 (65700), 320 (shoulder), 443 (11000). HRMS (EI): *m/z* (%): 456.1 (60), calcd for $\text{C}_{20}\text{H}_{36}\text{P}_4\text{Fe}$: 456.1100, found: 456.1117.

Received: October 23, 2008

Published online: January 13, 2009

Keywords: cyclobutadiene ligands · density functional calculations · iron · phosphorus · sandwich complexes

- [1] C. Elschenbroich, *Organometallchemie*, Teubner, Wiesbaden, **2008**, pp. 446–449.
- [2] *Metallocenes* (Eds.: A. Togni, R. L. Halterman), Wiley-VCH, Weinheim, **2008**.
- [3] a) A. Fürstner, K. Majima, R. Martin, H. Krause, E. Kattnig, R. Goddard, C. W. Lehmann, *J. Am. Chem. Soc.* **2008**, *130*, 1992; b) A. Fürstner, R. Martin, H. Krause, G. Seidel, R. Goddard, C. W. Lehmann, *J. Am. Chem. Soc.* **2008**, *130*, 8773, and references therein.
- [4] H. C. Longuet-Higgins, L. E. Orgel, *J. Chem. Soc.* **1956**, 1969.
- [5] G. F. Emerson, L. Watts, R. Pettit, *J. Am. Chem. Soc.* **1965**, *87*, 131.

- [6] D. Seyferth, *Organometallics* **2003**, *22*, 2.
- [7] J. D. Fitzpatrick, L. Watts, G. F. Emerson, R. Pettit, *J. Am. Chem. Soc.* **1965**, *87*, 3254.
- [8] Derivatives of **A** or the related compound [$\text{CpCo}(\eta^4\text{-C}_4\text{H}_4)$] have been employed as constituents of fascinating carbon-rich molecular objects such as conjugated polymers and star-shaped molecules, cf. U. H. F. Bunz, *Top. Curr. Chem.* **1999**, *201*, 131.
- [9] a) P. Binger, B. Biedenbach, R. Schneider, M. Regitz, *Synthesis* **1989**, 960; b) D. Himmel, M. Seitz, M. Scheer, *Z. Anorg. Allg. Chem.* **2004**, *630*, 1220.
- [10] a) D. Böhm, F. Knoch, S. Kummer, U. Schmidt, U. Zenneck, *Angew. Chem.* **1995**, *107*, 251; *Angew. Chem. Int. Ed.* **1995**, *34*, 198; b) F. W. Heinemann, S. Kummer, U. Seiss-Brandl, U. Zenneck, *Organometallics* **1999**, *18*, 2021.
- [11] To our knowledge, the only other homoleptic diphosphacyclobutadiene complex is the 18-electron species $[\text{Ni}(\eta^4\text{-P}_2\text{C}_2\text{Bu}_2)_2]$: T. Wetling, G. Wolmershäuser, P. Binger, M. Regitz, *J. Chem. Soc. Chem. Commun.* **1990**, 1541.
- [12] a) J. F. Nixon, *Coord. Chem. Rev.* **1995**, *145*, 201; b) M. Regitz, O. J. Scherer, *Multiple Bonds and Low Coordination Phosphorus Chemistry*, Thieme, Stuttgart, **1990**; c) K. B. Dillon, F. Mathey, J. F. Nixon, *Phosphorus: The Carbon Copy*, Wiley, Chichester, **1998**; d) F. Mathey, *Angew. Chem.* **2003**, *115*, 1616; *Angew. Chem. Int. Ed.* **2003**, *42*, 1578.
- [13] a) C. Ganter, *Chem. Soc. Rev.* **2003**, *32*, 130; b) J. Bai, A. V. Virovets, M. Scheer, *Science* **2003**, *300*, 781.
- [14] Rare examples of homoleptic cyclobutadiene complexes: a) H. Hoburg, R. Krause-Goeing, R. Mynott, *Angew. Chem.* **1978**, *90*, 138; *Angew. Chem. Int. Ed.* **1978**, *17*, 123; b) H. Hoburg, C. Froehlich, *J. Organomet. Chem.* **1981**, *213*, C49.
- [15] DFT calculations were performed using ADF2007.01, E. J. Baerends, J. Autschbach, A. Bérces, F. M. Bickelhaupt, C. Bo, P. M. Boerrigter, L. Cavallo, D. P. Chong, L. Deng, R. M. Dickson, D. E. Ellis, M. van Faassen, L. Fan, T. H. Fischer, C. Fonseca Guerra, S. J. A. van Gisbergen, J. A. Groeneveld, O. V. Gritsenko, M. Grüning, F. E. Harris, P. van den Hoek, C. R. Jacob, H. Jacobsen, L. Jensen, G. van Kessel, F. Kootstra, E. van Lenthe, D. A. McCormack, A. Michalak, J. Neugebauer, V. P. Nicu, V. P. Osinga, S. Patchkovskii, P. H. T. Philipsen, D. Post, C. C. Pye, W. Ravenek, P. Ros, P. R. T. Schipper, G. Schreckenbach, J. G. Snijders, M. Solà, M. Swart, D. Swerhone, G. te Velde, P. Vernooij, L. Versluis, L. Visscher, O. Visser, F. Wang, T. A. Wesolowski, E. M. van Wezenbeek, G. Wiesener, S. K. Wolff, T. K. Woo, A. L. Yakovlev, T. Ziegler, SCM, Theoretical Chemistry, Vrije Universiteit, Amsterdam, The Netherlands. The exchange–correlation potential is based on the GGA exchange functional OPTX (N. C. Handy, A. J. Cohen, *Mol. Phys.* **2001**, *99*, 403) in combination with the non-empirical PBE (J. P. Perdew, K. Burke, M. Ernzerhof, *Phys. Rev. Lett.* **1996**, *77*, 3865; OPBE), and an uncontracted triple-zeta valence-plus-2-polarization STO (TZ2P) basis set was used for all atoms. See the Supporting Information for details.
- [16] R. Wolf, A. W. Ehlers, J. C. Slootweg, M. Lutz, D. Gudat, M. Hunger, K. Lammertsma, *Angew. Chem.* **2008**, *120*, 4660; *Angew. Chem. Int. Ed.* **2008**, *47*, 4584.
- [17] a) W. W. Brennessel, V. G. Young, Jr., J. E. Ellis, *Angew. Chem.* **2002**, *114*, 1259; *Angew. Chem. Int. Ed.* **2002**, *41*, 1211; b) W. W. Brennessel, R. E. Jilek, J. E. Ellis, *Angew. Chem.* **2007**, *119*, 6244; *Angew. Chem. Int. Ed.* **2007**, *46*, 6132.
- [18] G. Becker, G. Gresser, W. Uhl, *Z. Naturforsch. B* **1981**, *36*, 16.
- [19] CCDC 704610 (**K2**) and 704611 (**3**) contain the supplementary crystallographic data for this paper. These data can be obtained free of charge from The Cambridge Crystallographic Data Centre via www.ccdc.cam.ac.uk/data_request/cif.
- [20] a) B. A. Goodman, J. B. Raynor, *Adv. Inorg. Chem. Radiochem.* **1970**, *13*, 135; b) “The Organometallic Chemistry of Rh-, Ir-, Pd-, and Pt-Based Radicals: Higher Valent Species”: B. de Bruin, D. G. H. Hetterscheid, A. J. J. Koekoek, H. Grützmacher, *Prog. Inorg. Chem.* **2007**, *55*, Chapter 5, p. 247.
- [21] See the Supporting Information for details.
- [22] A. Cecon, S. Santi, L. Orian, A. Bisello, *Coord. Chem. Rev.* **2004**, *248*, 683.